Structural Engineering and Mechanics, *Vol. 54, No. 6 (2015) 1111-1133*
DOI: http://dx.doi.org/10.12989/sem.2015.54.6.1111

Rebar corrosion effects on structural behavior of buildings

İsa Yüksel*

Department of Civil Engineering, Bursa Technical University, Yıldırım Campus, 16330 Bursa, Turkey

(Received October 3, 2014, Revised January 26, 2015, Accepted March 26, 2015)

Abstract. Rebar corrosion in concrete is one of the main causes of reduction of service life of reinforced concrete buildings. This paper presents the influence of rebar corrosion on the structural behavior of reinforced concrete (RC) buildings subjected to strong earthquake ground motion. Different levels of rebar corrosion scenarios were applied on a typical four story RC frame. The deteriorated conditions as a result of these scenarios include loss in cross-sectional area and loss of mechanical properties of the reinforcement bars, loss in bond strength, and loss in concrete strength and its modulus of elasticity. Dynamic analyses of the frame with different corrosion scenarios are performed with selected strong earthquake ground motion records. The influences of degradation in both concrete and reinforcement on structural behavior are investigated by comparing the various parameters of the frame under different corrosion scenarios with respect to each other. The results show that the progressive deterioration of the frame due to rebar corrosion causes serious structural behavior changes such as change in failure mode. The intensity, propagation time, and extensity of rebar corrosion have very important effects on the level of degradation of steel and concrete, as well as on the earthquake behavior of the structure.

Keywords: earthquake; frame; rebar corrosion; reinforced concrete

1. Introduction

Rebar corrosion is one of the most important mechanisms adversely affecting structural durability and the structural behavior of reinforced concrete (RC) structures. Structural performance and serviceability assessment of RC structures should account for the time-dependent variation of the structural response due to the associated to corrosion degradation mechanisms. Generally, durability problems such as rebar corrosion are not considered in the design phase of many low-rise concrete frame structures commonly used. However, rebar corrosion and concrete deterioration as a result of this phenomenon may weaken RC structures over time. As a result, such structures are more vulnerable to future earthquake hazards, especially in highly seismic regions. The main consequences of rebar corrosion are reductions of effective cross-section, concrete strength due to cracking and spalling, modulus of elasticity, bond degradation, and reduction of the ductility of the reinforcement steel (Rodriquez *et al*. 2002). Rebar corrosion adversely affects both the structural performance of a RC member and the entire structural system. Corrosion influences

*Corresponding author, Associate Professor, E-mail: isa.yuksel@btu.edu.tr

http://www.techno-press.org/?journal=sem&subpage=8 ISSN: 1225-4568 (Print), 1598-6217 (Online)

the properties of the reinforcing steel in two ways. First, there is a loss of the reinforcement's cross-sectional area. This can be tolerated with the overstrength of the section in the case of low-level corrosion. The second effect of corrosion on structural behavior is related to cracking and spalling, which is the loss of the concrete around bar due to expansion caused by corrosion products. Spalling creates two difficulties, which are loss of bond strength and loss of concrete section, which is more critical when the section that is spalling off is in the compression region. This will reduce the capacity of the member since all the concrete in the compression region is used to resist compression forces.

The aim of this paper is to evaluate the effects of rebar corrosion on the earthquake behavior of RC buildings. The reduction of cross-sectional area, cracking and spalling of the concrete cover, variations in the mechanical properties of the reinforcing steel, bond degradation, and force-deformation characteristics of the member due to degradation are selected as basic variables. Sectional analysis is performed on both corroded and un-corroded states of critical sections. Different probable corrosion scenarios are included to represent corroded structural systems in practice. Behaviors of corroded systems are compared with respect to the structural behavior of the un-corroded state. There are many analytical and experimental studies considering rebar corrosion; however, little work has been done the effects of all of the above variables on the structural behavior of RC structures exposed to the effects of earthquakes.

2. Past studies about rebar corrosion effects on structures

The corrosion rate of rebar in RC structural elements has been believed to be too slow to be of concern. This belief is coming from the high alkalinity of the pore solution in the concrete, and the barrier provided by the cover concrete against the aggressive agents from the outside environment. However the degradation process of concrete over time is a consequence of the chemical, biological, physical and environmental attacks that the structure may suffer during its service lifetime. Concrete cracks at the end of the degradation process as a result of exceeding the tensional strain capacity of concrete. Rebar corrosion in RC structures is a major reason for structural durability degradation. Over recent decades, intensive research has been carried out on the influence of rebar corrosion on the structural performance of RC structures.

Rebar corrosion can be initiated due to chloride ingress in concrete or due to depassivation of the protective thin oxide film of the steel reinforcement through the action of carbon dioxide from the atmosphere (Apostopoulos 2013). The durability of RC structures and its service life is widely affected by rebar corrosion (Demis *et al.* 2014). Propagated corrosion causes concrete cracks in both longitudinal and tangential directions, and these cracks may accelerate further corrosion with subsequent continuous deterioration of structural performance (Yüksel 2013). These deteriorations have negative effects on structural behavior, such as premature collapse or changing of collapse mechanisms of the structure from ductile to fragile. The corrosion process results in a rust layer on the steel reinforcement surface that causes the increase of the volume of steel due to the chlorides of Fe_2O_3, responsible for cracking and spalling of the cover of concrete. An important result of the rebar corrosion for RC structures is the decrease in bond strength (Demis *et al*. 2010). Existence of perfect bond between steel and concrete is one of the basic assumptions to provide the reinforced concrete behavior. The degradation of bond strength causes an increase in the global drift ratio of RC structures that needs to be considered in non-linear seismic performance analyses. At the same time, corrosion reduces the cross-sectional area of the reinforcement. The reinforcement might

buckle before reaching their yield capacity as a result of this reduction in cross-sectional area. Moreover, the energy dissipation capacity is reduced during an earthquake, which causes more brittle behavior (Yalçıner 2012).

Material properties of reinforcement steel bars are also changed due to the corrosion process, and its ductility in terms of strain will be reduced. The ductility of a corroded bar depends on exposure environment, i.e. carbonation or chlorides (Hanjari 2010). Ductility is an important parameter to take into account regarding inelastic behavior in seismic design. It is also required to allow redistribution of forces from highly stressed to less stressed areas. Rebar corrosion affects member ductility. For instance, if a significant amount of the area of a reinforcing bar is lost due to pitting corrosion, there is a possibility that the bar will fracture rather than yield. To avoid premature fracture, minimum levels of ductility are specified in codes and standards for reinforcement. For example, the BS EN 10080 criterion for elongation at the maximum load is 2.5% for normal grade reinforcement.

Tuutti's (1982) model is widely used for the definition of the time frame associated with the initiation and propagation of the corrosion process. Deterioration can be distinguished into two stages in this model as a function of exposure time. The first stage is called the corrosion initiation phase and involves the attack of aggressive agents. The second stage is called the propagation phase and leads to damage in concrete as well as cross-sectional reduction of reinforcing bars. Although corrosion damage is not observed in the first phase, gradually increasing damage will be observed in propagation phase. Revathy *et al.* (2009) showed that as corrosion intensity is increased, the axial load carrying capacity and ductility of columns is decreased. Other researchers (Almusallam *et al.* 1996, Rodriquez *et al*. 1997, Mangat *et al.* 1999, Mohammed *et al.* 2004) have also shown that the failure mode changes from ductile to fragile for structural elements and structural systems exposed to rebar corrosion. Pitting corrosion may involve a significant reduction in steel ductility and it may induce a brittle behavior in the reinforcement bar. Almusallam (2001) showed that steel behavior might become brittle in tensile tests of corroded bars in the case of 13% mass loss. Palsson and Mirza (2002) showed that corroded bars retrieved from an abandoned bridge demonstrated brittle failure in tension tests. Apostolopoulos and Papadakis (2008) reported that ductility reduction is a function of cross-section loss. The ultimate strain of steel can be related to the damage index (Biondini and Vergani 2012). Ying *et al.* (2012) showed that higher corrosion levels and higher axial loads result in less stable hysteretic loops with more severe strength and stiffness degradations and worse ductility. Ghosh and Padgett (2012) determined important changes in seismic fragility along the service life of RC bridges due to corrosion deterioration. They concluded that other components of bridges also showed rapid increases in fragility. Kato *et al.* (2006) stated that corrosion of the main reinforcement had an influence on the load carrying capacity and ductility of the RC beams, while corrosion of the stirrup especially had an influence on ductility. Also, deterioration of bonding loss between the main reinforcement and the concrete became important in improving the accuracy of the evaluation of the ductility of the corroded RC beam.

Designers assume that a perfect bond exists between reinforcement steel bars and the surrounding concrete. This assumption ensures compatibility of deformations of both concrete and reinforcement steel. However, this is not the actual scenario, due to bonding loss problems. Bond is influenced by many variables, and its interaction with shear influences the member behavior significantly. Therefore, it is very important to understand the bond deterioration mechanism and to estimate the bond strength of corroded RC beams. Bond strength is a function of the concrete tensile strength. Many researchers (Cabrera 1996, Lee *et al*. 2002, Chung *et al*. 2008, Demis *et al*

2010) have investigated the relationship between corrosion level and bond behavior. Some empirical and experimental equations have been proposed relating corrosion level with bond strength. Auyeung *et al.* (2000) indicated that after 2% diameter loss, there is a reduction in flexural capacity. The structural behavior of columns or beams exposed to propagated corrosion is similar to plain concrete because the bond strength has almost completely disappeared. On the other hand, Ghandehari *et al.* (2000) showed that the rebar corrosion effect on bond strength is negligible when a high percentage of confining transverse steel is used. Chung *et al*. (2008) stated that the bond strength initially increases up to a maximum value but eventually decreases at greater levels of corrosion. Wu (2012) proposed a model that was developed to predict the residual flexural capacity of corroded RC members. He concluded that the bonding loss between steel and concrete is the main factor in the mechanical degradation of flexural capacity.

Andrés *et al*. (2007) observed a 60% reduction in the flexural load-carrying capacity at about 10% of $X_{AVER}/r0$ ratio, where r0 is the rebar radius and X_{AVER} is average corrosion penetration. They concluded that the maximum rebar pit depth was the most important parameter affecting the reduction of flexural load capacity in corroded beams. Mangat and Elgarf (1999) found a 24% reduction at almost the same degree of corrosion. They showed that the breakdown of bond at the steel/concrete interface caused marked reductions in flexural strength. Bertagnoli *et al.* (2006) reported that the position of the corroded areas in relation to the reinforcement layout and reinforcement geometry also plays a relevant role in defining the failure mechanism in corroded RC structures. Gu *et al.* (2010) showed that the degradation of the load-carrying capacity and stiffness of beams increased with the increase in the degree of corrosion. The loss in cross-sectional area and the degradation of the mechanical properties of the corroded rebar were found to be the major reasons for the decrease in the load-carrying capacity of the beams, while the reduction in stiffness was mostly attributed to the bonding loss. The type of corrosion has important effects on bond strength. Pitting corrosion has a more negative effect than uniform corrosion (Coronelli 2004, Kivell *et al*. 2011a, Kivell *et al*. 2011b).

There are a limited number of studies about bond-slip behavior of corroded reinforcing steel under cyclic loading. Fang (2006) stated that there was a maximum reduction in bond strength in the case of 5% corrosion of the reinforcing steel under cyclic loading. Also, Fang *et al*. (2006) concluded that severe corrosion will cause significant reduction in bond capacity under cyclic loading. Saito *et al*. (2007) showed that electrochemical corrosion caused premature buckling of column longitudinal reinforcement, reducing the effectiveness of confinement reinforcement.

O'Flaherty *et al*. (2010) stated that reinforced concrete beams show a loss in stiffness with increasing corrosion of the main and shear steel reinforcement. Corrosion of transverse and longitudinal reinforcements could change the failure mode of the corroded member, which is very important for structures. Ou *et al*. (2010) stated that as the corrosion exposure increased, the failure mode changed from flexural failure to flexural-shear failure. Additionally, owing to a smaller bar size, the transverse reinforcement showed a higher percentage weight loss and maximum pit depth for a given corrosion duration. Also, they stated that the ultimate drift, ductility, plastic rotation capacity, and energy dissipation increased in the initial stage of corrosion and then decreased with a further increase in the corrosion level.

Based on the past studies about corrosion and capacity of structural elements there is need of determine relations between all consequences of rebar corrosion and the overall structural behavior of the RC buildings. To understand these interactions is very important for existing old RC buildings that under consideration of seismic performance evaluation. The present study with a numerical example could be useful to clarify the effect of rebar corrosion on the structural behavior of RC buildings.

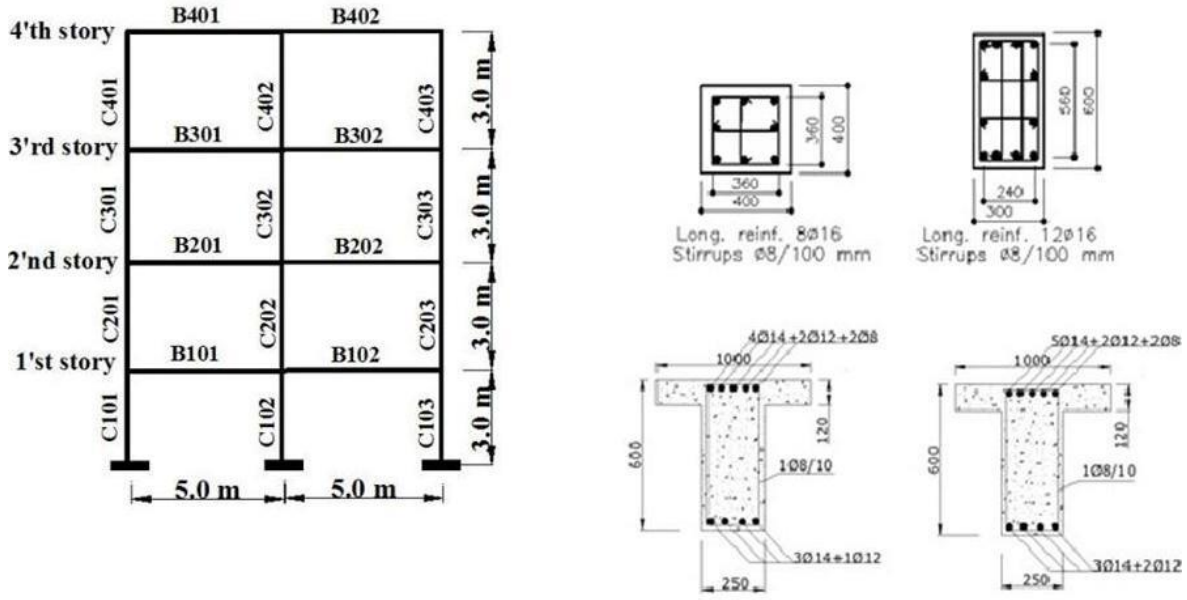

(a) Frame labeling and dimensions

(b) Column and beam sections with reinforcement layout

Fig. 1 Frame labeling and typical sections of structural elements

3. Numerical example

3.1 Selected structural model

A typical four-story residential building frame is selected in order to apply an evaluation methodology for the influence of rebar corrosion under strong earthquake ground motion. The frame is considered to be a representation of regular low-rise RC structures in practice. The model (Fig. 1(a)) was designed with dead and live loads, on all beams, equal to 13.5 kN/m and 10.5 kN/m respectively. It is designed according to the requirements of the current TEC-2007 and TBC-500 with design peak ground acceleration of 0.4g. A class Z3 soil, similar to class C soil of FEMA-356 (FEMA 2000) defined in TEC-2007, is selected, which corresponds to a medium stiff sand-gravel site having an equivalent shear wave velocity of 200-400 m/s, and a site soil layer thickness between 15 m and 50 m is chosen. Spectrum characteristic periods of Z3 soil are T_A=0.15 s, and T_B=0.60 s. The story heights and bay widths are selected as 3 m and 5 m, respectively. Fig. 1(b) shows the typical structural member sections and the reinforcement details. Exterior columns had a cross-section of 400 mm×400 mm and contained eight longitudinal reinforcements with a nominal diameter of 16 mm. The interior column had a cross-section of 600 mm × 300 mm, where 600 mm is the depth and 300 mm is the width. It has twelve longitudinal reinforcements whose diameter is 16 mm. Both types of columns have tie reinforcement of 8 mm in diameter with 100 mm spacing. Reinforcement layouts were identical on all stories. The concrete compressive strength of the control system is assumed to be 25 MPa. S420 type of hot-worked steel is used for longitudinal and tie reinforcements. Mechanical and chemical properties of these bars were shown in the Turkish Standard TS708-Steel bars for concrete (TSE 2010). The

Table 1 Earthquake ground motions

Earthquake	Station Place	Peak acc. (g)	Component	Sampling interval (sec)
Düzce, 12/11/1999	Düzce Meteorological Station	0.524	E-W	0.05
Erzincan, 13/03/1992	Erzincan Meteorological Station	0.471	E-W	0.05
Kocaeli, 17/08/1999	Kocaeli Meteorological Station	0.220	E-W	0.005
Imperial Valley, 15/10/1979	CDMG Sta. 942	0.439	El Centro array #6	0.005
Kobe, 16/01/1995	KJMA	0.821	Kobe KJM 000	0.02
Northridge, 17/01/1994	24279 Newhall Fire Sta.	0.590	Northridge NWH360	0.02
Tabas, 16/09/1978	9101 Tabas	0.836	TAB-LN	0.02
Cape Mendocino, 25/04/1992	89156 Petrolia	0.589	PET000	0.02
Morgan Hill, 24/04/1984	CDMG Sta. 57217	1.298	CYC285	0.005

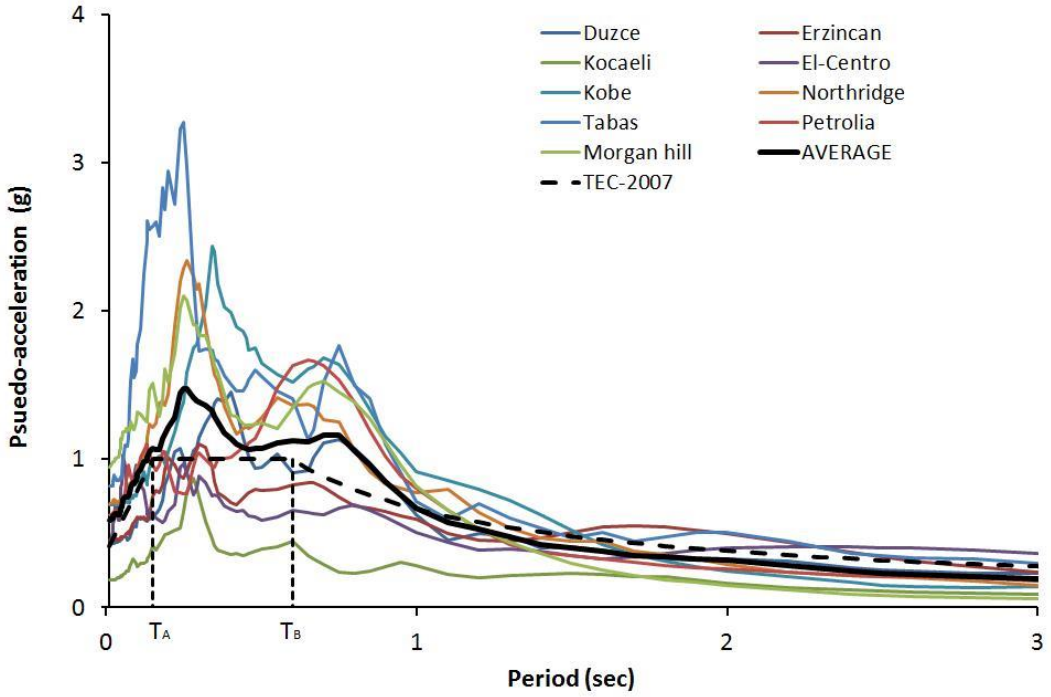

Fig. 2 Five percent damping elastic response spectra of input ground motions

minimum specified yield strength (R_e) of the steel according to TS708 is 420 MPa and the minimum elongation to failure is 10%. Ultimate strength (R_m) and elastic modulus of the steel bars are 500 MPa, and 210 GPa respectively. Maximum allowable percentage by weight of carbon, sulfur, and phosphorus are 0.45, 0.050, and 0.050 respectively. The concrete cover in all members

was assumed to be 30 mm. The structural model is fixed at the base nodal points, while other nodes are free with respect to rotation and translation. The first mode period is calculated as 0.61 seconds, and the mass participation factor is determined to be 0.831.

3.2 Input ground motions

The earthquake damage of a structure is sensitive to the factors that are provided structural capacity and the input earthquake intensity level. Because of the importance of the input earthquake intensity level, some real earthquake records are selected from nine different strong earthquakes. These records are used in dynamic analysis of the frame. The selected input ground motions are shown in Table 1. These records were downloaded from two sources-the website of the Pacific Earthquake Engineering Research Center (PEER 2009) and the website of the Republic of Turkey Prime Ministry Disaster & Emergency Management Presidency. Most of the selected records are near fault ground motions that can impose larger response demands on lower stories of weak structures compared with far fault ground motions. Fig. 2 shows the elastic pseudo-acceleration response spectra of the records (with 5% damping) and their median values. The thick lines in Fig. 2 show the mean acceleration response spectrum. The dotted thick lines in Fig. 2 show the design acceleration spectrum with respect to the peak ground acceleration of 0.4g and Z3 type soil specified in TEC-2007. In Fig. 3, T_A=0.15 seconds, and T_B=0.6 seconds, - are the spectral response periods.

3.3 Material characteristics and corrosion scenarios

Eight different corrosion scenarios are considered in addition to the sound condition of the frame. These scenarios contain low and high states of intensity and propagation times of corrosion. It should be noted that intensity and propagation time are the parameters investigated. 10 and 20 years are selected to represent low and high propagation time. 1 and 4 μA/cm^2 corrosion intensity values are selected to represent low and high intensity. Extensity of the corrosion on the structure is a third parameter that its effect is also investigated. Two basic extents of corrosion are selected. In the first, uniform corrosion affects the whole frame, while in the second corrosion affects only the first story's beams and columns. Basic scenarios are noted as S1-10-1, S1-20-1, S2-10-4, and S2-20-4, which are scenarios that depend on corrosion intensity and propagation time. The first term in the scenario code shows the name of the scenario, the second term shows propagation time in years, and the third term shows corrosion intensity. To evaluate the extensity of corrosion on the structure, all of these scenarios are repeated for the case that corrosion affects only the first story. These scenario codes have "OFS" at the end as fourth term. The scenario representing the reference (control) state is denoted as S0. All scenarios are shown in Table 2 in detail.

Rebar corrosion damages could be seen in different ways. As intensity and propagation time of rebar corrosion increases, the diameter of reinforcement steel is reduced. At the same time, in the case of severe corrosion, the mechanical properties of reinforcing steel are negatively affected. Moreover, bond strength is reduced or completely disappeared depending on the rate of corrosion. As a result, cracking and spalling of cover concrete is observed. The effects of corrosion on reinforcing steel, on concrete, and on bond strength should be considered for each scenario. The reduced diameter of reinforcing bar after propagation time is calculated using Eq. (1).

$$\Phi(t) = \Phi_0 - 2P_x = \Phi_0 - 2i_{corr}\kappa(t - t_{in}) \tag{1}$$

Table 2 Corrosion scenarios

Scenario code	Extensity on the frame	Propagation time, t_p (year)	Intensity, i_{corr}, (μA/cm^2)
S0	Whole frame	0	0
S1-10-1	Whole frame	10	1
S1-10-1 OFS	At only first story	10	1
S1-20-1	Whole frame	20	1
S1-20-1 OFS	At only first story	20	1
S2-10-4	Whole frame	10	4
S2-10-4 OFS	At only first story	10	4
S2-20-4	Whole frame	20	4
S2-20-4 OFS	At only first story	20	4

Table 3 Revised characteristics of reinforcement bars for each scenario

Scenario code	Nominaldiameter (mm)	After corrosion					
		Dia. (mm)	Mass loss (%)	Yield stress f_y,(Mpa)	Ultimate stress, f_u,(Mpa)	Ultimate strain, ε_u	Elastic moduli E_s, (Mpa)
S1-10-1	8	7.77	5.72	390.2	516.4	0.089	191426
	12	11.77	3.83	400.1	527.5	0.093	194256
	14	13.77	3.29	402.9	530.7	0.094	195070
	16	15.77	2.88	405.0	533.1	0.094	195682
	20	19.77	2.31	408.0	536.4	0.096	196540
S1-20-1	8	7.54	11.26	361.3	483.7	0.078	183105
	12	11.54	7.58	380.5	505.4	0.085	188624
	14	13.54	6.52	386.1	511.6	0.087	190222
	16	15.54	5.72	390.2	516.4	0.089	191426
	20	19.54	4.59	396.1	523.0	0.091	193121
S2-10-4	8	7.07	21.85	306.2	421.4	0.057	167218
	12	11.07	14.87	342.6	462.5	0.071	177697
	14	13.07	12.82	353.3	474.6	0.075	180773
	16	15.07	11.26	361.3	483.7	0.078	183105
	20	19.07	9.06	372.8	496.7	0.082	186403
S2-20-4	8	6.14	41.02	206.4	308.6	0.020	138474
	12	10.14	28.54	271.4	382.0	0.044	157188
	14	12.14	24.76	291.1	404.3	0.052	162865
	16	14.14	21.85	306.2	421.4	0.057	167218
	20	18.14	17.70	327.8	445.8	0.065	173452

In Eq. (1) $\phi(t)$ (mm) is the diameter at time t, ϕ_0 (mm) the nominal diameter, t_{in} (years) the time for corrosion initiation at the rebar surface, i_{corr} (μA/cm^2) the current corrosion density, κ a conversion factor of μA/cm^2 into mm/year for steel (equal to 0.0116), and P_x (mm) is the average value of the attack penetration (Berto *et al.* 2008). Eqs. (2)-(5) developed from experimental results by Lee and Cho (2009) are used in this study. Mechanical and chemical properties of steel which are used in this study are similar to steel used to develop Eqs. (2)-(5). These equations relate corrosion percentage with loss of the mass due to rebar corrosion.

Table 4 Revised characteristics of concrete for corrosion scenarios

Scenario code	C101, C201, C301, C401, C103, C203, C303, C403 (40×40 cm)		C102, C202, C302, C402 (30×60 cm)		All beams, (25×60 cm)	
	f_c (MPa)	E_c (MPa)	f_c (MPa)	E_c (MPa)	f_c (MPa)	E_c (MPa)
S0	25	25000	25	25000	25	25000
S1-10-1	23.75	24367	20.76	22782	17.17	20715
S1-20-1	23.13	24044	19.31	21972	15.14	19457
S2-10-4	22.28	23600	17.58	20961	12.98	18016
S2-20-4	21.19	23016	15.59	19743	10.80	16434

$$\sigma_{cy} = (1 - 1.98(\frac{\Delta_w}{100}))\sigma_{sy} \tag{2}$$

$$\sigma_{ct} = (1 - 1.57(\frac{\Delta_w}{100}))\sigma_{st} \tag{3}$$

$$E_{cs} = (1 - 1.15(\frac{\Delta_w}{100}))E_{ss} \tag{4}$$

$$\delta_c = (1 - 2.59(\frac{\Delta_w}{100}))\delta_s \tag{5}$$

Where σ_{cy} is the yield strength of steel after corrosion; Δ_w the corrosion percentage; σ_{sy} the nominal yield strength of steel; σ_{ct} the ultimate strength of steel after corrosion; σ_{st} the nominal ultimate strength of steel; E_{cs} the elastic modulus of steel after corrosion; E_{ss} the nominal elastic modulus of steel; δ_c the elongation after corrosion; δ_s the nominal elongation of steel. At Tables 3 and 4, the revised properties of the reinforcement and concrete for each scenario are respectively shown.

Nominal yield stress, ultimate stress, ultimate strain, and modulus of elasticity for the reinforcement steel are 420 MPa, 550 MPa, 0.1%, and 2×10^5 MPa, respectively. Compressive strength and elastic moduli reductions are considered in the revision of concrete characteristics for scenarios. The nominal concrete compressive strength is assumed as 25 MPa. Moduli of elasticity of sound and cracked concrete are calculated from the equation given in TEC-2007 as follows

$$E_C = 5000\sqrt{f_c} \tag{6}$$

3.4 Analyses

Before the dynamic analyses of the scenarios took place, cross-sectional analysis of beam and column end sections were performed using XTRACT V.3.0.9 (Imbsen 2011). Reduction in diameter of reinforcement steel, revised properties of reinforcement bars and concrete were used as input data for the cross-sectional analyses. The Mander model (Mander *et al*. 1988) was used for confined and unconfined concrete. Bilinear steel model with strain hardening was used for the reinforcement steel. Longitudinal and hoop reinforcement were defined specifically for each

Table 5 Hysteretic modelling parameters in IDARC2D for beam and column elements

Parameter	Nominal value for S0	Selected value for $i_{corr=1}$	Selected value for $i_{corr=4}$	Typical limit values
Stiffness degrading (α)	15	10	8	4 :Severe 10:Moderate 15:Mild 200:No degrading
Ductility-based strength decay (β)	0.15	0.30	0.45	0.60:Severe 0.30:Moderate 0.15:Mild 0.01:No degrading
Hysteretic energy-based strength decay (β2)	0.08	0.30	0.45	0.60:Severe 0.30:Moderate 0.08:Mild 0.01:No degrading
Slip or crack closing (γ)	0.40	0.25	0.15	0.05:Severe 0.25:Moderate 0.40:Mild 1.00:No degrading

corroded beam or column sections. Constant axial forces were applied on column sections calculated from G+0.3Q load combination in moment curvature analyses. However axial forces were ignored for beam sections in these analyses. As a result, normal force-moment interaction diagrams or moment-curvature diagrams were defined specifically for each section because of different levels of corrosion damage.

Incremental dynamic analyses were performed on the sound state and corroded states of the frame to establish the corrosion effects on the structural behavior of the system. The selected input ground motions were applied to the frame model, and various nonlinear response parameters were determined. The damping ratio of the model in all scenarios was assumed as 2%. IDARC2D (2009) is used for inelastic dynamic analysis of corroded and un-corroded RC frames to observe the changes in structural behavior. The load-deformation of the structure is simulated by versatile hysteretic models, which are implemented in the program and are mainly controlled by parameters indicating the stiffness degradation, strength deterioration, and pinching of the hysteretic loops. The damage index developed by Park *et al*. (1984) has been incorporated into the program and is used to estimate the accumulated damage sustained by the components of the structure, by each story, and by the entire building. A global value of the damage index can be used to characterize damage in the entire RC frame (Sadjadi *et al*. 2007). There are two options for defining the material properties for each element in IDARC2D. Either the program will generate the envelopes for the elements, or the program requires complete moment curvature envelope data to be provided by the user. The moment curvature envelope determined from the software XTRACT is used as the data input to the program in this study. Reduced stiffness of the members is considered in the moment curvature envelope. The hysteretic values should characterize strength deterioration, stiffness degradation, and pinching behavior for the columns and beams. These parameters are considered for each corrosion scenario. Table 5 shows selected hysteretic modeling parameters.

Damage index comparisons are also included in this study. Park *et al*. (1987) suggested a damage index for damage analysis of reinforced concrete structures; the index is considered in

Table 6 Suggested interpretations by Park *et al*. (1987) for the overall damage index

DI<0.10	No damage or localized minor cracking
0.10≤DI<0.25	Minor damage-light cracking throughout
0.25≤DI<0.40	Moderate damage-severe cracking, localized spelling
0.40≤DI<1.0	Severe damage-crushing of concrete, reinforcement exposed
DI≥1.0	Collapsed

IDARC in modified form. The modified model by Kunnath *et al*. (1992) is shown in Eq. (7) as follows

$$DI = \frac{\theta_m - \theta_r}{\theta_u - \theta_r} + \frac{\beta}{M_y \theta_u} E_h \tag{7}$$

where θ_m is the maximum rotation attained, θ_u is the ultimate rotation capacity of the section, θ_r is the recoverable rotation at unloading, M_y is the yield moment, E_h is the dissipated energy in the section, and β is the strength degrading parameter. The component damage index is the largest damage index of the end sections of the structural element. In order to calculate the overall damage index, the story damage index should be calculated first. Both the story and overall damage indexes are shown in Eqs. (8)-(9) as follows

$$DI_{story} = \sum_{i=1}^{n} (DI)_{component} \left[\frac{E_i}{\sum_{i=1}^{n} E_i} \right]_{component} \tag{8}$$

$$DI_{overall} = \sum_{i=1}^{n} (DI)_{story} \left[\frac{E_i}{\sum_{i=1}^{n} E_i} \right]_{story} \tag{9}$$

where E_i is the total absorbed energy by the component or the i^{th} story. Park *et al*. (1987) suggested the following interpretations for the damage index given in Table 6.

4. Results and discussion

4.1 Sectional analyses

Typical changes are observed in the moment-curvature relationship of the column sections generated for corrosion scenarios with revised material characteristics and hysteretic modeling parameters. As an example, Fig. 3 shows the moment-curvature relationship at the base section of column C102. As intensity and propagation time of rebar corrosion increases, the after yielding plateau of moment-curvature curve is shortened. This result shows that deformation capacities of the corroded sections are dramatically decreased. Also moment capacities of these sections are

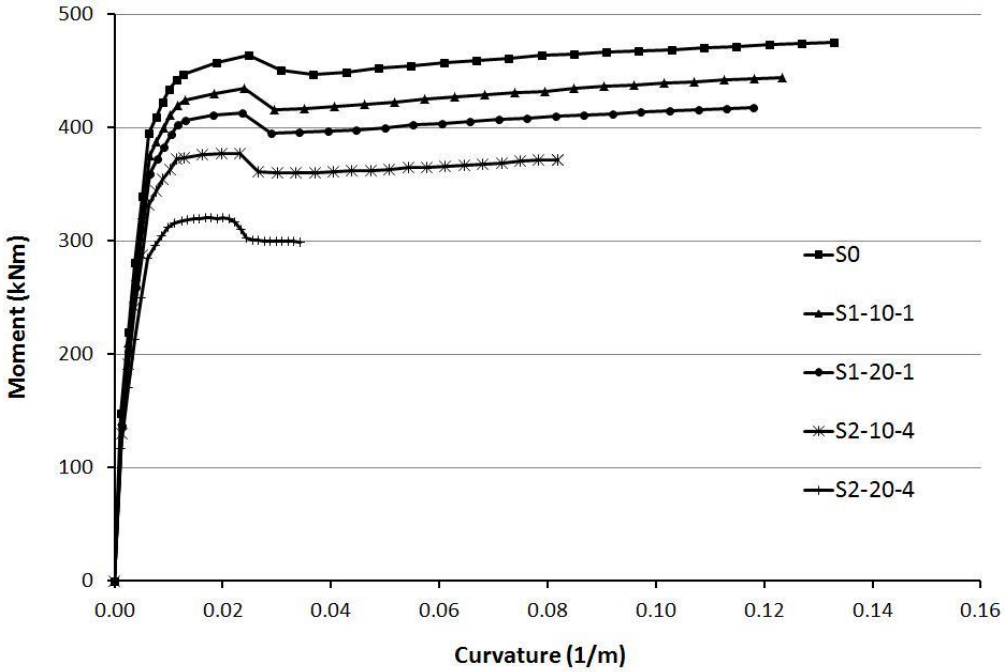

Fig. 3 Moment-curvature relationship of base section of column C102 with respect to corrosion scenarios

decreased. Sectional ductility, defined as ultimate curvature to effective yield curvature, is decreased as corrosion intensity and propagation time increases. Sectional ductility of the same column in scenario S0, which is reference scenario, is about 391% greater than the sectional ductility attained at the scenario S2-20-4 in which the sectional ductility capacity is 4.71. The reason for this decrease is the degeneration of the column cross-section. As corrosion propagates, corrosion products create an internal pressure between the cover concrete and the reinforcement bar. This causes concrete cracks in radial and tangential directions. Revised values for concrete and reinforcement bar are defined in order to simulate the degeneration of the reinforcement bar and surrounding concrete. As a result, yield and ultimate moments of the section are decreased.

Fig. 4 shows the column interaction diagram of the same column C102, and there are also typical decreases in axial force and moment capacity of the column section as the amount of corrosion increases. These moment and axial load carrying capacity reductions have negative effects on member and system behavior. Moreover, stirrup corrosion increases the rate of reduction in load carrying capacity of column. Stirrup corrosion has a great effect on confinement affectivity. When stirrups do not perform as expected, the unsupported length of longitudinal reinforcement increases which may results in premature buckling of the longitudinal reinforcement. Tapan and Aboutaha (2011) found similar results when they investigated structural effects of corrosion on the residual load-carrying capacity of reinforced concrete bridge columns under several deterioration cases. Demirtaş (2008) investigated the effects of corrosion on RC columns under constant axial load and cyclic lateral loads. He found out that corrosion damage had an adverse effect on moment-curvature and interaction diagrams of RC columns especially under high rate of corrosion.

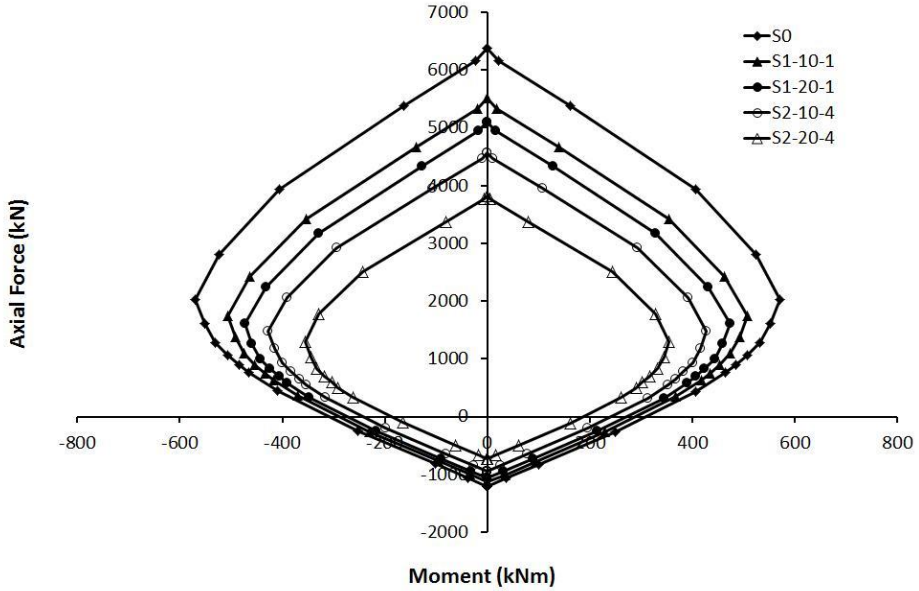

Fig. 4 Moment axial force interaction diagrams of base section of column C102 for selected corrosion scenarios

4.2 System behavior

4.2.1 Drift ratio

The interstorey drift depends on the stiffness of the moment resisting frame followed by plastic deformation and the mode shape of vibration. Maximum drift ratios of story 1 obtained from average of nine strong earthquakes with respect to different corrosion scenarios are shown in Fig. 5. The minimum drift ratio of the first story is obtained in scenario S0. A gradual increase in drift ratio is observed in scenarios in which corrosion exposure occurs only in the first story as compared with scenarios that correspond to corrosion exposure in the whole structure. The maximum drift ratio is obtained in scenario S2-20-4 OFS, which corresponds to corrosion exposure only on the first floor at high intensity and long propagation time. Since corrosion degeneration is accumulated on this story, the rigidity of this story is decreased with respect to other stories. As a result, interstorey drift is maximized on this story. Especially in the case of high corrosion intensity, the extensity of corrosion is more important. The difference of drift ratio between S2-20-4 and S2-20-4 OFS scenarios shows that damage accumulation on the first story causes higher drift ratio.

Fig. 6 shows average of maximum drift ratios obtained from nine strong earthquakes with respect to different corrosion scenarios on the fourth story. In contrast to Fig. 5, there is a gradual decrease in the drift ratio of the fourth story in scenarios in which corrosion exposure occurs only on the first story. Since structural damage is largely accumulated on the first story, this accumulation causes the failure mechanism on this story.

Variations of drift ratio with respect to stories are shown in Fig. 7. It could be seen that the values of interstorey drifts are increased in the lower stories and decreased in the upper ones. Typical differences between story 4 and 1, are also evident in Fig. 7. Since column stiffness of

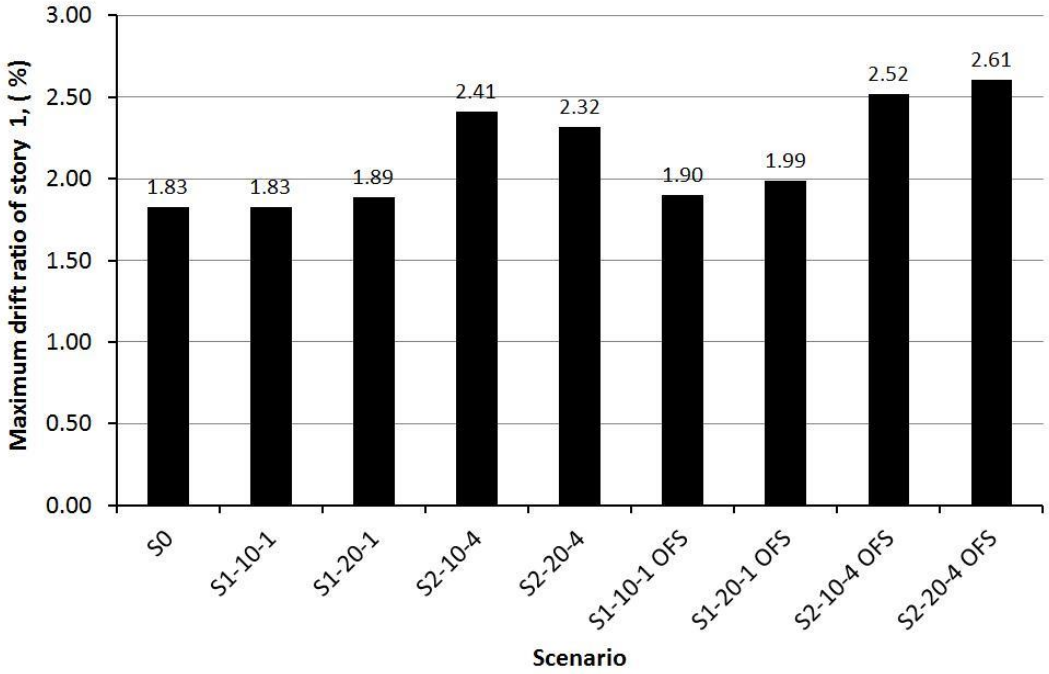

Fig. 5 Maximum drift ratios of story 1 obtained from average of nine strong earthquakes with respect to different corrosion scenarios

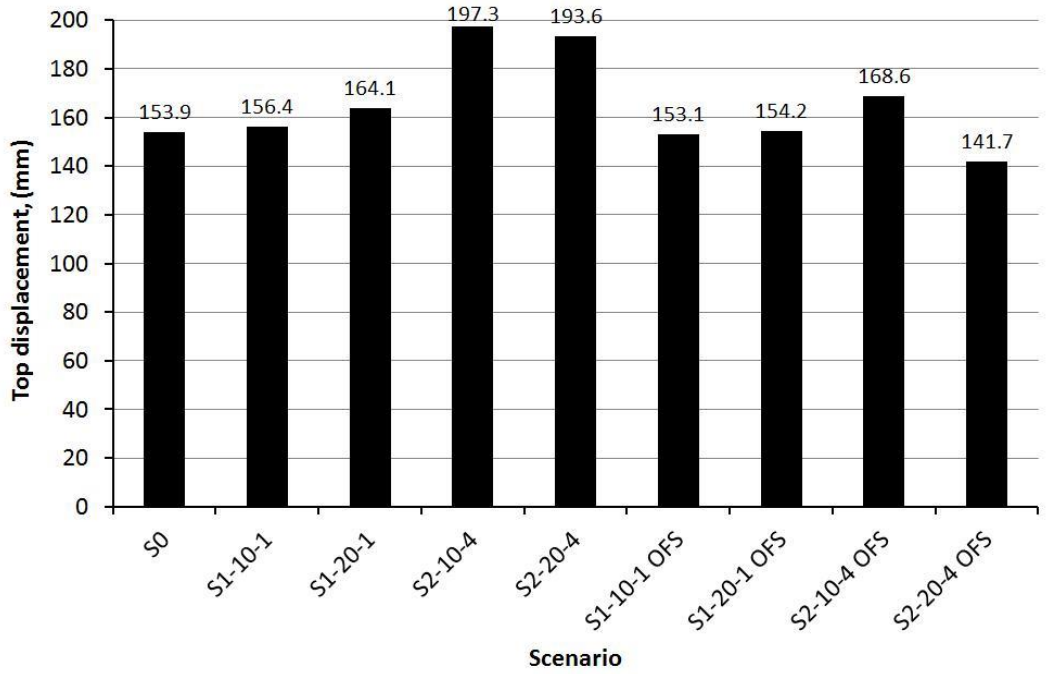

Fig. 6 Averages of maximum drift ratios obtained from nine strong earthquakes with respect to different corrosion scenarios on the fourth story

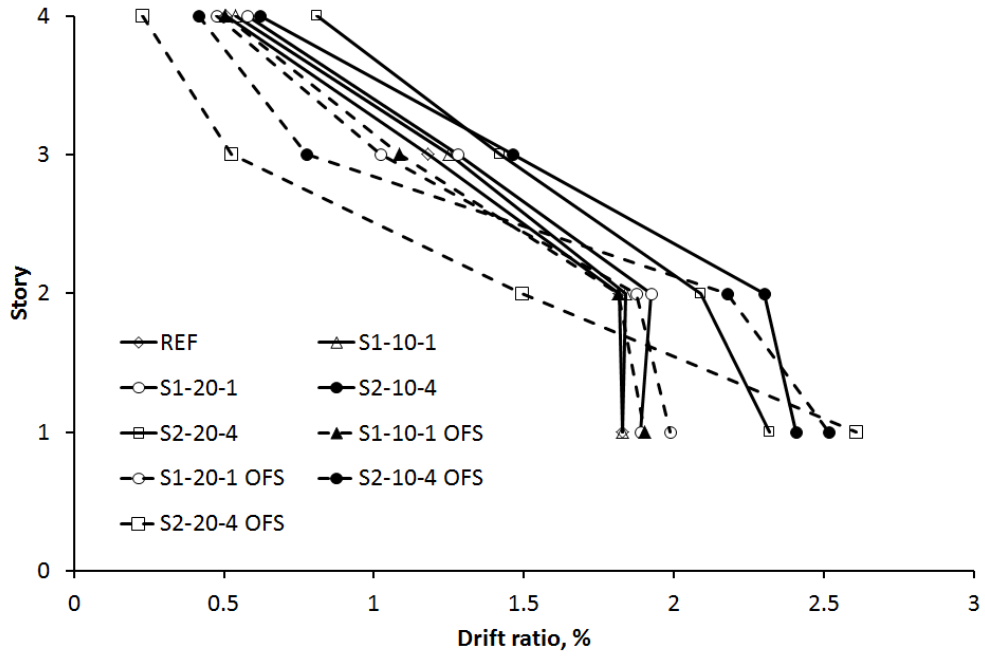

Fig. 7 Variations of drift ratio with respect to stories

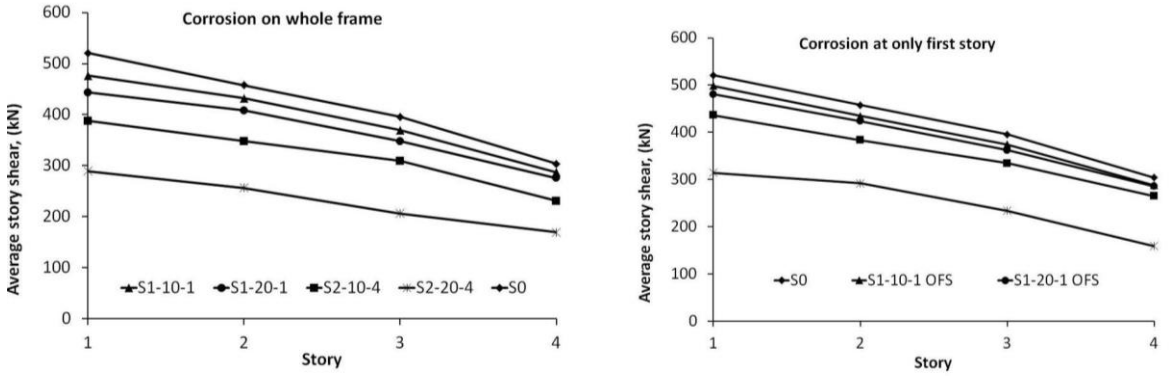

(a) On whole frame (b) On only first story

Fig. 8 Distribution of average story shear in case of corrosion effects

story 1 decreased with respect to the un-corroded case, the drift ratio of this story is increased. However when corrosion exposures occur throughout the whole structure, the stiffness of the all stories is generally decreased. Therefore, the behavior pattern of the system did not changed, but the drift ratio values are generally increased for the whole structure. The first mentioned case is more dangerous, since the first story has become weak story which is not a preferable case.

4.2.2 Story shear

Distribution of story shear forces on the frame for the average of nine strong earthquake effects

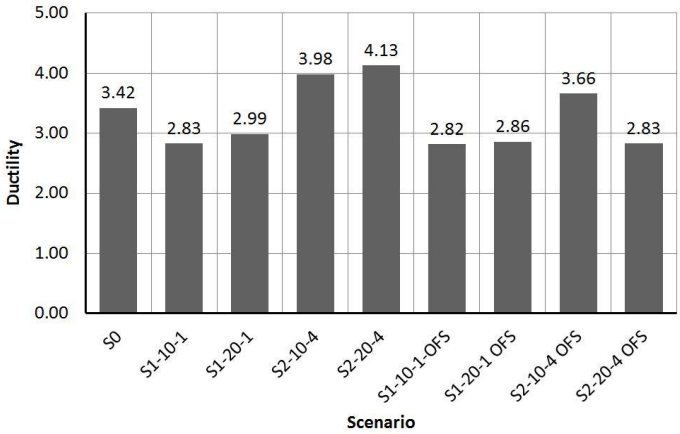

Fig. 9 Average values of ductility demand of scenarios for the nine strong earthquake motions

is shown in Fig. 8. Different corrosion effect scenarios on the whole frame and on the first story only are shown in Figs. 8(a) and 8(b) respectively. A similar trend is observed in both of these figures. An increase in story shear force in the lower stories and a decrease in the upper stories is evident. Story shear force values are decreasing in all stories as corrosion effect increases. This variation is typical for the scenarios S2-20-4 and S2-20-4 OFS. Compared to scenario S0, only 56% of the base shear force is acting on the first story, in scenario S2-20-4 and 60% in scenario S2-20-4 OFS. There is a 4% increase in the first story's shear force as there is a 4% decrease in fourth story's shear force, which is decreased to from 56% to 52% for the scenario S2-20-4 OFS.

4.2.3 Ductility demand

The yield displacement of the frame was assumed to be the time of the first column's yielding. Structural ductility was calculated as the ratio of the ultimate top displacement to the yield displacement of the frame. Fig. 9 shows ductility demand with respect to corrosion scenarios. The maximum ductility demand is observed in scenario S2-20-4 in which corrosion damage is maximum. On the other hand, the structural ductility demand is decreased in scenario S2-20-4 OFS in which corrosion damage is accumulated only on the first story and deformation demand is maximum on the first story. Therefore, the structural system ductility demand is decreased. The reason of this is that the system ductility is defined as the ratio of ultimate displacement to yield displacement of the top story. In fact, in this case, the story ductility demand is more important than the structural ductility demand. The local ductility demands need to be limited to the ductility capacity of the cross-section used. Deformation capacity of the columns and beams on the first story govern the structural behavior, as can be seen also in the final states of the frame in Fig. 12 which shows final states of the frame for the Düzce earthquake for three scenarios.

4.2.4 Damage index

The overall damage index distribution obtained from the selected earthquakes with respect to corrosion scenarios are summarized in Fig. 10. In order to better understand the difference between them, only two scenarios having the most mass loss in their categories are shown with the reference scenario in this figure. Generally, the maximum overall damage index is obtained in scenario S2-20-4. It can be seen from Fig. 10 that the overall damage index increases 2-3 times for

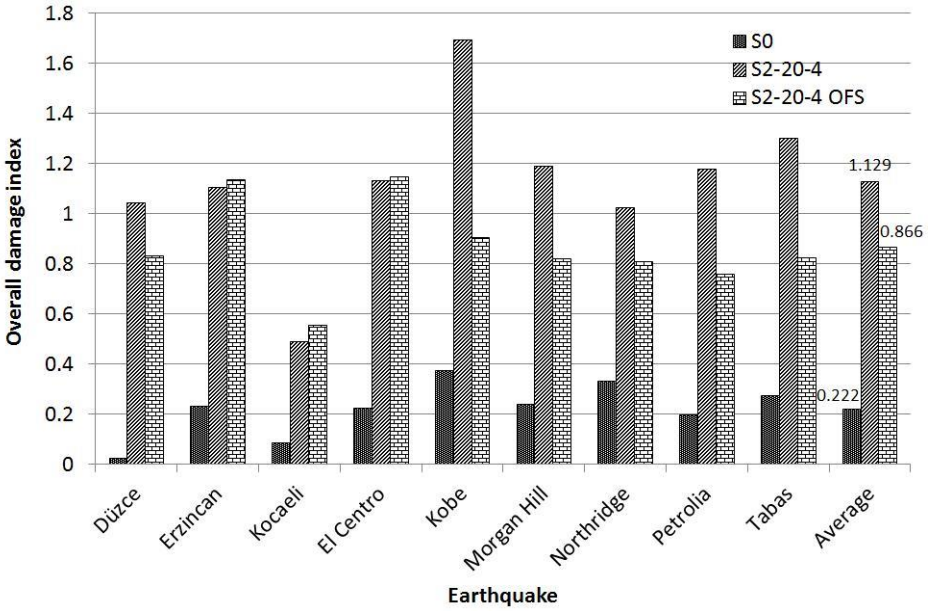

Fig. 10 Overall damage index for different earthquakes and scenarios

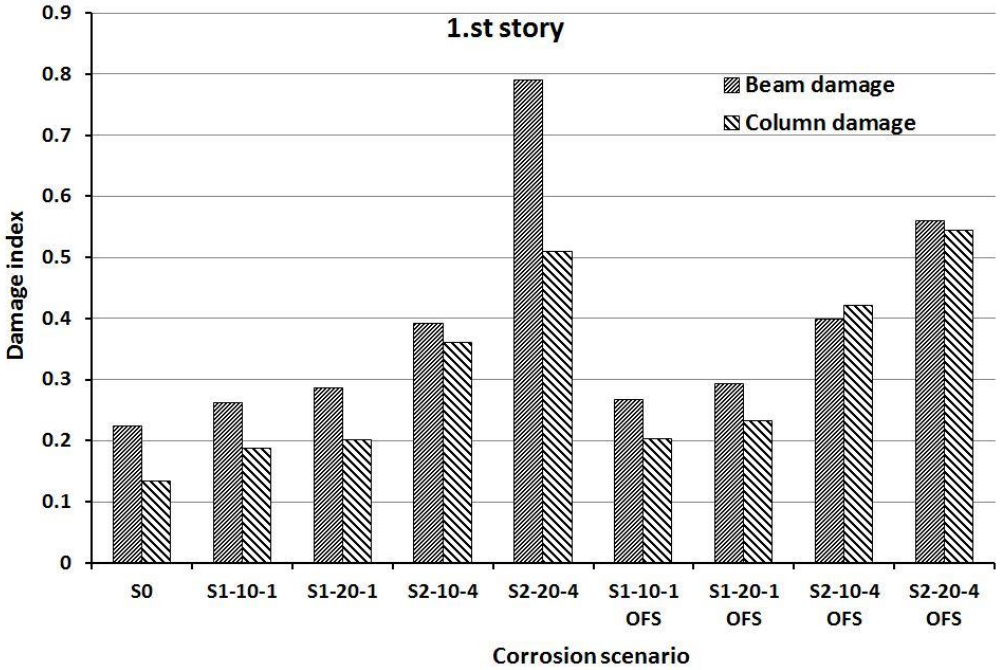

Fig. 11 Variation of beam and column damage indexes w.r.t. corrosion scenarios at the first story

the different strong earthquake motions in these two scenarios (S2-20-4 and S2-20-4 OFS) corresponding to extensive corrosion with high intensity and long propagation times. As a result, extensive corrosion results in extremely deteriorated structural behavior. According to the

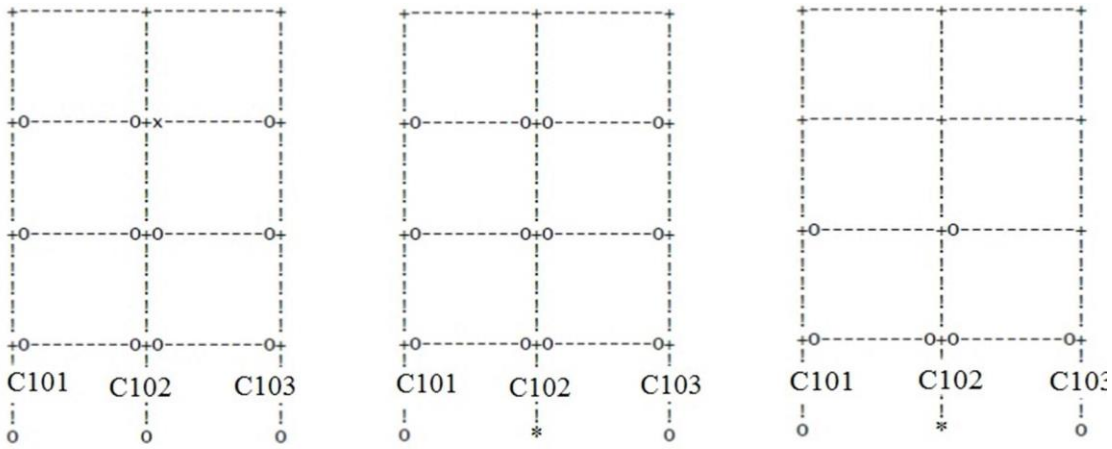

(a) S0 (b) S2-20-4 (c) S2-20-4 OFS

Notation: x =Cracking for concrete or initial yield for steel; o=Plastic hinge developed;
*=Local failure (exceed criteria)

Fig. 12 Final state of the frame for the Düzce earthquake for three scenarios

interpretations shown in Table 6, moderate damage will be expected from selected earthquakes for the scenario S0. On the other hand, severe damage or collapse level should be expected for the corrosion scenarios S2-20-4 and S2-20-4 OFS. The average value of overall damages for scenario S2-20-4 obtained from nine strong earthquakes is determined as 1.129, which means that the system will collapse according to Table 6. The same value for the scenario S2-20-4 OFS is 0.866, implying severe damage for the system. However, the same value for the un-corroded system is only 0.222, meaning that no damage or localized minor cracking will occur. It should be noted that accumulation of damage on the first story may change the system failure mode. Therefore, the overall damage index values should not be evaluated alone. Fig. 11 shows the beam and column damage index distribution in different corrosion scenarios for the first story. It is worth noting that when corrosion affects the whole story, beam damage index are higher than column index for all scenarios for the first story. However column damage index is very near or higher than the beam damage index for the scenarios corresponding to corrosion effects only to first story of the structure. This case shows that when corrosion affects only the first story, results in similar structural behavior when corrosion affects the whole structure. In practice the case of the corrosion affects foundation, basement, and ground floor is often encountered.

4.2.5 Plastic hinge formations and final states of frames

Plastic hinge formation sequence and plastic deformations on the frame system were analyzed under the earthquake action. Column plastic hinges affect the frame system behavior more than the beam plastic hinges. The first plastic hinges are formed at the beam ends for all earthquake actions. Then column plastic hinges are formed at the bottom end of first floor columns. Therefore, the un-corroded system (S0) showed strong column-weak beam behavior, as expected in earthquake-resistant structures. Energy dissipation occurred with beam sway mechanism before failure. However, especially in scenarios S2-20-4 and S2-20-4 OFS, some important variations at

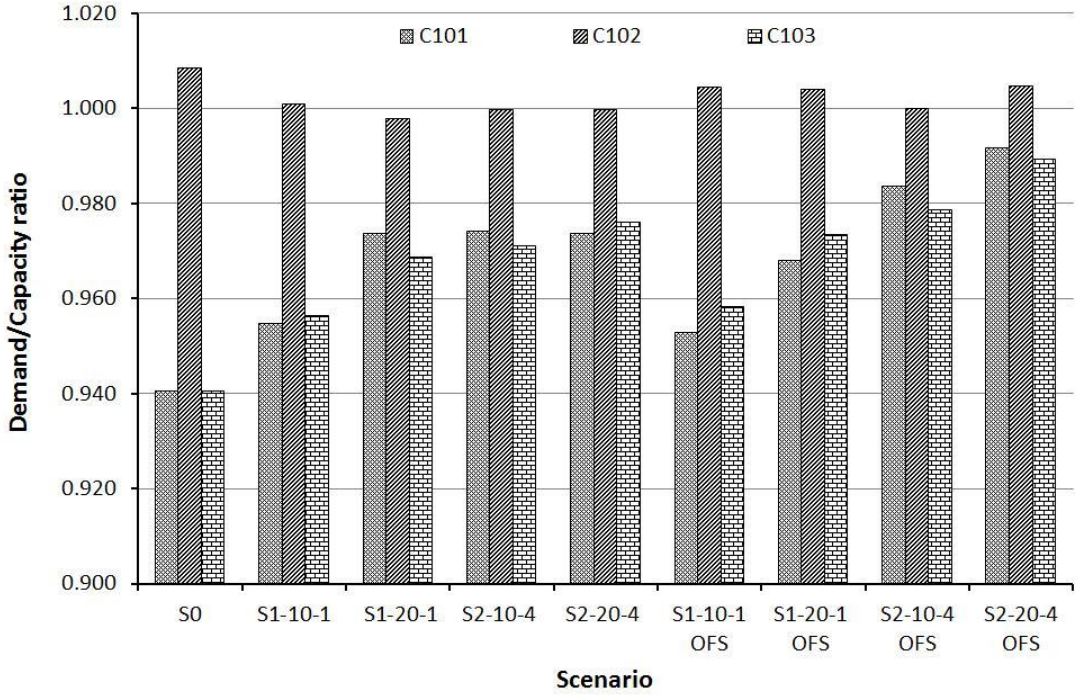

Fig. 13 Demand to capacity ratios with respect to scenarios for columns at the first story

the order of plastic hinge formations were observed which affect the global system behavior. The plasticization sequences in scenarios S2-20-4 and S2-20-4 OFS are typically different than other scenarios. Moreover, there are considerable differences between these two scenarios. Since corrosion affects only the first floor columns and beams, deformation capacity of this story and its corresponding members are higher than the others. Therefore plastic hinge formations begin and deformation capacities of the plasticized sections are used earlier on this story than the other stories. This difference causes relatively earlier failure as compared to the un-corroded system. For example, Fig. 12 shows the final state of the frame for the Düzce earthquake. The final state in S0 (un-corroded state) is similar to behavior of ductile systems (Fig. 12(a)). After plastic hinges occurred in 11 beams, column plastic hinges occurred at the bottom ends of columns C101, C102, and C103. Fig. 12(b) shows the final state of the frame for scenario S2-20-4. Local failure is observed at the bottom end of column C102. On the other hand, unlike Fig. 12(b), the number of beam plastic hinges formed in Fig. 12(c) is less than the number of beam plastic hinges formed in Fig. 12(a) and Fig. 12(b). This shows that early local failures occurred at column sections in Fig.12 (a). This system did not dissipate energy by means of beam plastic hinges before formation of column plastic hinges in scenario S2-20-4 OFS. As a result, rebar corrosion caused the non-preferred behavior under strong earthquake effects.

4.2.6 Demand to capacity ratio of critical columns

The moment demand to capacity ratio is a good measure of how much of the moment capacity of the column is used for a considered action. A demand to capacity ratio greater than one indicates member failure. The moment demand to capacity relationship of three critical columns at

the first story is shown in Fig. 13. Moment capacity of the bottom end of interior column C102 is completely used in all scenarios and plastic hinges are formed on this section in all scenarios. The same ratio for columns C101 and C103 are greater than 0.940, which means that they are used almost to their capacity. An increasing trend on moment demand to capacity ratio was observed as corrosion rate and intensity were increased for all columns considered in Fig. 13. It is worth noting that scenarios in which corrosion affects only the first story has a greater demand to capacity ratio than scenarios in which corrosion effects the whole frame. This result shows that local corrosion may have equal or greater effects on the structural behavior of the system. As the bottom ends of columns yield, lateral displacement of the structure is increased.

5. Conclusions

This study evaluated the rebar corrosion effects on structural behavior of buildings with a numerical example where a comparative evaluation of the earthquake behavior of a regular multistory frame structure took place. The structure was exposed to different rebar corrosion scenarios under different strong earthquake motion effects. Earthquake behaviors of RC frames are sensitive to rebar corrosion damages, as the level of damage is dependent on the degree and extent of corrosion in the structure. The degree of corrosion is governed by intensity and propagation time of it. Rebar corrosion has adverse effects on properties of reinforcement steel and concrete, bond strength between concrete and reinforcement steel, and deformation characteristics of structural elements such as beams and columns. It was found out that these parameters adversely affect earthquake behavior of the frame structure. Its strength and ductility capacities were reduced. In case of high level of corrosion, its failure mode also could be switched from ductile to fragile. Especially, extensive high-level corrosion affecting only the first story probably causes an unwanted non-ductile collapse mechanism under strong earthquake motions. Local corrosion, such as rebar corrosion affecting only the first story, can cause similar results with extensive high-level corrosion. Therefore it should be also interpreted like high-level extensive rebar corrosion. Moreover rebar corrosion damage should be certainly considered in evaluation of structural performance of existing structures in highly seismic regions. Overall, further studies are required in order to consider the slippage of corroded reinforcement and bond strength in order to evaluate corrosion damages more precisely.

References

Almusallam, A.A. (2001), "Effect of degree of corrosion on the properties of reinforcing steel bars", *Constr. Build. Mater.*, **15**(8), 361-368.

Almusallam, A.A., Al-Gahtani, A.S., Aziz, A.R., Dakhil, F.H. and Rasheeduzzafar. (1996), "Effect of reinforcement corrosion on flexural behaviour of concrete slabs", *J. Mater. Civil Eng.*, **8**(3), 123-127.

Apostolopoulos, C.A., Demis, S. and Papadakis, V.G. (2013), "Chloride-induced corrosion of steel reinforcement -mechanical performance and pit depth analysis", *Constr. Build. Mater.*, **38**(1), 139-146.

Apostolopoulos, C.A. and Papadakis, V.G. (2008), "Consequences of steel corrosion on the ductility properties of reinforcement bar", *Constr. Build. Mater.*, **22**(12), 2316-2324.

Auyeung, Y.B., Balaguru, P. and Chung, L. (2000), "Bond behavior of corroded reinforcement bars", *ACI Mater. J.*, **97**(2), 214-220.

Bertagnoli, G., Mancini, G. and Tondolo, F. (2006), "Bond deterioration due to corrosion and actual bearing

capacity", *Proceedings of the 2nd International Congress, Session 15-Durability of Concrete Structures*, Naples, June.

Berto, L., Seatta, A., Simioni, P. and Vitaliani, R. (2008), "Nonlinear static analyses of RC frame structures: influence of corrosion on seismic response", *Proceedings of the 8th. World Congress on Computational Mechanics (WCCM8) and 5th European Congress on Computational Methods in Applied Sciences and Engineering (ECCOMAS 2008)*, Venice, June-July.

Biondini, F. and Vergani, M. (2012), "Damage modeling and nonlinear analysis of concrete bridges under corrosion", *6th International Conference on Bridge Maintenance, Safety and Management (IABMAS)*, Stresa, July.

Cabrera, J.G. (1996), "Deterioration of concrete due to reinforcement steel corrosion", *Cemment Concrete Compos.*, **18**(1), 47-59.

Chung, L., Kim, J.J. and Seong, Y. (2008), "Bond strength prediction for reinforced concrete members with highly corroded reinforcing bars", *Cemment Concrete Compos.*, **30**(7), 603-611.

Coronelli, D. and Gambarova, P. (2004), "Structural assessment of corroded reinforced concrete Beams: Modeling guidelines", *J. Struct. Eng.*, **130**(8), 1214-1224.

Demis, S., Efstathiou, M.P. and Papadakis, V.G. (2014), "Computer-aided modelling of concrete service life", *Cement Concrete Compos.*, **47,** 9-18.

Demis, S., Pilakoutas, K. and Apostolopoulos, Ch. (2010), "Effect of corrosion on bond strength of steel and non-metallic reinforcement", *Mater. Corros.*, **61**(4), 328-331.

Fang, C. (2006), "Bond strength of corroded reinforcement under cyclic loading", *Mag. Concrete Res.*, **58**(7), 437-446.

Fang, C.Q., Gylltoft, K., Lundgren, K. and Plos, M. (2006), "Effect of corrosion on bond in reinforced concrete under cyclic loading", *Cement Concrete Res.*, **36**(3), 548-555.

Ghandehari, M., Zulli, M. and Shah, S.P. (2000), "Influence of Corrosion on bond degradation in reinforced concrete", *Proceedings of the ASCE Engineering Mechanics Conference*, Austin, TX, May.

Ghosh, J. and Padgett, J.E. (2012), "Impact of multiple component deterioration and exposure conditions on seismic vulnerability of concrete bridges", *Earthq. Struct.*, **3**(5), 649-673.

Gu, X.L., Zhang, W.P., Shang, D.F. and Wang, X.G., (2010), "Flexural behavior of corroded reinforced concrete beams", *Earth and Space 2010: Engineering, Science, Construction, and Operations in Challenging Environments*, Honolulu, March.

Hanjari, K.Z. (2010), "Structural behaviour of deteriorated concrete structures", Ph.D. Dissertation, Chalmers University of Technology, Gothenburg.

IDARC2D Version 7.0 (2009), A Program for the Inelastic Damage Analysis of Structures, Developed by A.M. Reinhorn, H. Roh, M. Sivaselvan, S.K. Kunnath, R.E. Valles, A. Madan, C. Li, R. Lobo and Y.J. Park, State University of New York.

Imbsen Software System, (2001), "XTRACT-Cross Sectional analysis of components", Sacramento.

Kato, E., Iwanami, M. and Yokota, H. (2006), "Deterioration in ductility of rc beams with corroded reinforcement", *Proceedings of the 2nd International Congress, Session 15-Durability of Concrete Structures*, Naples, June.

Kivell, A., Palermo, A. and Scott, A. (2011a), "Effects of bond deterioration due to corrosion in reinforced concrete", *Ninth Pacific Conference on Earthquake Engineering*, Auckland, April.

Kivell, A., Palermo, A. and Scott, A. (2011b), "Monotonic and cyclic bond testing of heavily corroded reinforcing high strength concrete", *9th International Symposium on High Performance Concrete*, Christchurch, August.

Kunnath, S.K., Reinhorn, A.M. and Lobo, R.F. (1992), "IDARC Version 3.0: A program for the Inelastic Damage Analysis of RC Structures", Report No. NCEER-92-0022, National Center for Earthquake Engineering Research, State University of New York at Buffalo, N.Y.

Lee, H.S. and Cho, Y.S. (2009), "Evaluation of the mechanical properties of steel reinforcement embedded in concrete specimen as a function of the degree of reinforcement corrosion", *Int. J. Fract.*, **157**(1-2), 81-88.

Lee, H.S., Noguchi, T. and Tomosawa, F. (2002), "Evaluation of the bond properties between concrete and

reinforcement as a function of the degree of reinforcement corrosion", *Cemment Concrete Res*., **32**(8), 1313-1318.
Mander, J.B., Priestley, M.J.N. and Park, R. (1988), "Theoretical stress–strain model for confined concrete", *J. Struct. Eng*., **114**(8), 1804-1826.
Mangat, P.S. and Elgarf, M.S. (1999). "Flexural strength of concrete beams with corroding reinforcement." *ACI Struct. J*., **96(**1), 149-158.
Mohammed, T.U., Hamada, H. and Yamaji, T. (2004), "Concrete after 30 years of exposure-Part II: Chloride ingress and corrosion of steel bars", *ACI Struct. J*., **101**(1), 13-18.
O'Flaherty, F.J., Mangat, P.S. and Lambert, P. (2010), "Influence of steel reinforcement corrosion on the stiffness of simply supported concrete beams", *IABMAS10: Proceedings of the fifth International IABMAS Conference*, Philadelphia, July.
Ou, Y.C., Tsai, L.L. and Chen, H.H. (2012), "Cyclic performance of large-scale corroded reinforced concrete beams", *Earthq. Eng. Struct. Dyn*., **41**(4), 593-604.
Palsson, R. and Mirza, M.S. (2002), "Mechanical response of corroded steel reinforcement of abandoned concrete bridge", *ACI Struct. J*., **99**(2), 157-162.
Park, Y.J., Ang, A.H.S. and Wen, Y.K. (1984), "Seismic damage analysis and damage-limiting design of r/c buildings, civil engineering studies", Technical Report No. SRS 516, University of Illionis, Urbana.
Park, Y.J., Ang, A.H.S. and Wen, Y.K. (1987), "Damage-limiting aseismic design of buildings", *Earthq. Spectra*, **3**(1), 1-26.
PEER (2014), Strong Motion Database, Website of the Pacific Earthquake Engineering Research Center, http://peer.berkeley.edu/peer_ground_motion_database/.
Republic of Turkey Prime Ministry Disaster & Emergency Management Presidency Earthquake Department (2014), Website of the National Strong motion Observation Network, http://kyh.deprem.gov.tr/ftpe.htm.
Revathy, J., Suguna, K. and Raghunath, P.N. (2009), "Effect of corrosion damage on the ductility performance of concrete columns", *Am. J. Eng. Appl. Sci*., **2**(2), 324-327.
Rodriquez, J., Ortega, L., Izquierdo, D. and Andrade, C. (2002), "Detailed assessment of concrete structures affected by reinforcement corrosion", *First Fib Congress*, Osaka, October.
Rodriguez, J., Ortega, L.M. and Casal, J. (1997), "Load carrying capacity of concrete structures with corroded reinforcement", *Constr. Build. Mater*., **11**(4), 239-248.
Sadjadi, R., Kianoush, M.R. and Talebi, S. (2007), "Seismic performance of reinforced concrete moment resisting frames", *Eng. Struct*., **29(**9), 2365-2380.
Saito, Y., Oyado, M., Kanakubo, T. and Yamamoto, Y. (2007), "Structural performance of corroded RC column under uniaxial compression load", *First International Workshop on Performance, Protection & Strengthening of Structures under Extreme Loading*, Whistler, August.
Tapan, M. and Aboutaha, R.S. (2011), "Effect of steel corrosion and loss of concrete cover on strength of deteriorated RC columns", *Constr. Build. Mater*., **25**(5), 2596-2603.
TBC-500-(2000), Requirements for design and construction of reinforced concrete structures, Turkish Standards Institute (TSE), Ankara, Turkey. (in Turkish)
TEC-2007-Turkish Earthquake-resistant Code, Specification for Buildings to Be Built in Seismic Zones, Ministry of Public Works And Settlement, Ankara, Turkey. (in Turkish)
Torres-Acosta, A.A., Navarro-Gutierrez, S. and Teran-Guillen, J. (2007), "Residual flexure capacity of corroded reinforced concrete beams", *Engineering Structures*, **29**(6), 1145-1152.
TS708 (2010), Steel for the reinforcement of concrete - Reinforcing steel, Turkish Standards Institute (TSE), Ankara, Turkey. (in Turkish)
Tuutti, K. (1982) "Corrosion of steel in concrete", CBI research report no 4.82. Swedish Cement and Concrete Research Institute, Stockholm, Sweden.
Wu, H. (2012), "Bond degradation and residual flexural capacity of corroded rc beams", Master Thesis, Ryerson University, Toronto.
Yalciner, H., Sensoy, S. and Eren, Ö. (2012), "Effect of corrosion damage on the performance level of a 25-year-old reinforced concrete building", *Shock Vib.*, **19**(5), 891-902.
Ying, M., Yi, C. and Jinxin, G. (2012), "Behavior of corrosion damaged circular reinforced concrete

columns under cyclic loading", *Constr. Build. Mater*., **29**(1), 548-556.
Yüksel, I. and Coşkan, S. (2013), "Earthquake response of reinforced concrete frame structures subjected to rebar corrosion", *Earthq. Struct.*, **5**(3), 321-341.

CC